

UC Berkeley

UC Berkeley Previously Published Works

Title

Biosynthesis of Isonitrile Lipopeptide Metallophores from Pathogenic Mycobacteria

Permalink

<https://escholarship.org/uc/item/3594q3hd>

Journal

Biochemistry, 62(3)

ISSN

0006-2960

Authors

Del Rio Flores, Antonio
Narayanamoorthy, Maanasa
Cai, Wenlong
[et al.](#)

Publication Date

2023-02-07

DOI

10.1021/acs.biochem.2c00611

Peer reviewed



HHS Public Access

Author manuscript

Biochemistry. Author manuscript; available in PMC 2023 February 08.

Published in final edited form as:

Biochemistry. 2023 February 07; 62(3): 824–834. doi:10.1021/acs.biochem.2c00611.

Biosynthesis of Isonitrile Lipopeptide Metallophores from Pathogenic Mycobacteria

Antonio Del Rio Flores,

Department of Chemical and Biomolecular Engineering, University of California, Berkeley, California 94720, United States

Maanasa Narayanamoorthy,

Department of Chemistry, University of California, Berkeley, California 94720, United States

Wenlong Cai,

Department of Chemical and Biomolecular Engineering, University of California, Berkeley, California 94720, United States

Rui Zhai,

Department of Chemical and Biomolecular Engineering, University of California, Berkeley, California 94720, United States

Siyue Yang,

Department of Chemistry, University of California, Berkeley, California 94720, United States

Yuanbo Shen,

Department of Chemistry, University of California, Berkeley, California 94720, United States

Kaushik Seshadri,

Department of Chemical and Biomolecular Engineering, University of California, Berkeley, California 94720, United States

Kyle De Matias,

Department of Chemical and Biomolecular Engineering, University of California, Berkeley, California 94720, United States

Zhaoqiang Xue,

Corresponding Author: Wenjun Zhang – Department of Chemical and Biomolecular Engineering, University of California, Berkeley, California 94720, United States; wjzhang@berkeley.edu.

Author Contributions

A.D.R.F designed all the experiments presented in this work, conducted cloning, in vitro biochemical assays, and chemical synthesis, analyzed the data, and wrote the manuscript. M.N. helped to purify protein, performed biochemical assays, and helped with chemical synthesis. W.C. aided in chemical synthesis and analyzed the NMR presented in this work. R.Z. helped with chemical synthesis and NMR analysis. Y.S. and S.Y. helped to purify protein and perform biochemical assays. K.S. and K.D.M. conducted site-directed mutagenesis on *scoE* and *Rv0097*, aided in biochemical assays, and performed protein purification. Z.X. aided with chemical synthesis. W.Z. designed the experiments, analyzed data, and wrote the manuscript.

Supporting Information

The Supporting Information is available free of charge at <https://pubs.acs.org/doi/10.1021/acs.biochem.2c00611>.

Experimental details, chemical synthesis schemes, primers utilized for plasmid construction, NMR spectra, and supplemental LC–HRMS data (PDF)

Complete contact information is available at: <https://pubs.acs.org/doi/10.1021/acs.biochem.2c00611>

The authors declare no competing financial interest.

Department of Chemical and Biomolecular Engineering, University of California, Berkeley, California 94720, United States

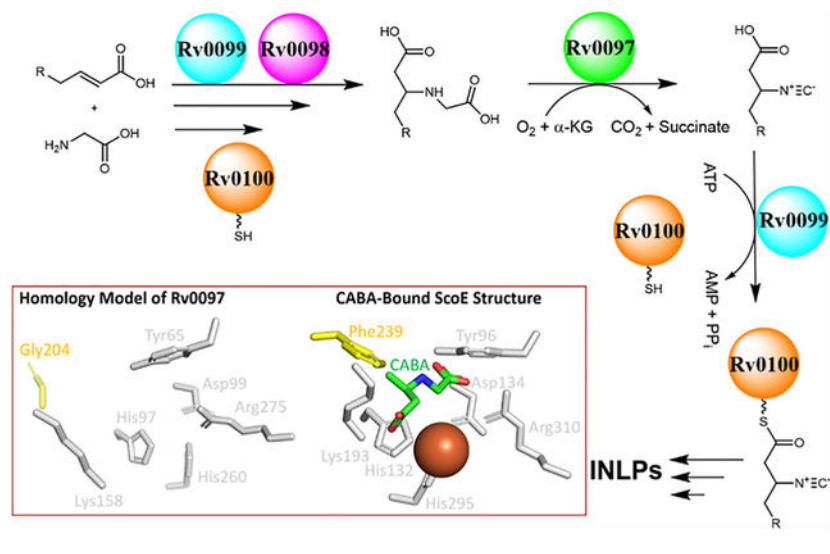
Wenjun Zhang

Department of Chemical and Biomolecular Engineering, University of California, Berkeley, California 94720, United States

Abstract

Isonitrile lipopeptides (INLPs) are known to be related to the virulence of pathogenic mycobacteria by mediating metal transport, but their biosynthesis remains obscure. In this work, we use in vitro biochemical assays, site-directed mutagenesis, chemical synthesis, and spectroscopy techniques to scrutinize the activity of core enzymes required for INLP biosynthesis in mycobacteria. Compared to environmental *Streptomyces*, pathogenic *Mycobacterium* employ a similar chemical logic and enzymatic machinery in INLP biosynthesis, differing mainly in the fatty-acyl chain length, which is controlled by multiple enzymes in the pathway. Our in-depth study on the non-heme iron(II) and α -ketoglutarate-dependent dioxygenase for isonitrile generation, including Rv0097 from *Mycobacterium tuberculosis* (*Mtb*), demonstrates that it recognizes a free-standing small molecule substrate, different from the recent hypothesis that a carrier protein is required for Rv0097 in *Mtb*. A key residue in Rv0097 is further identified to dictate the varied fatty-acyl chain length specificity between *Streptomyces* and *Mycobacterium*.

Graphical Abstract



INTRODUCTION

Natural products are biologically synthesized small molecules that intercede pivotal biological processes including, but not limited to signaling, interference competition, nutrient acquisition, biofilm formation, and virulence.¹⁻⁵ Such specialized metabolites are commonly decorated with unique functionalities, like the isonitrile, which behave as bioactive warheads by fulfilling critical ecological functions.^{6,7} Recently, a family of

isonitrile lipopeptides (INLPs) was discovered as metallophores, produced by a widely spread non-ribosomal peptide synthetase (NRPS)-encoding biosynthetic gene cluster (BGC) in actinobacteria (Figure 1A).⁸ Specifically, the INLP SF2768 was identified from various environmental *Streptomyces* species and was shown to behave as a chalkophore by mediating copper acquisition.^{9,10} The homologous INLP BGCs were also found to be conserved in the pathogenic *Mycobacterium* species, including *Mycobacterium tuberculosis* (*Mtb*) and *Mycobacterium marinum*, and recent studies suggested that INLPs in mycobacteria were also involved in metal transport, although the identity of the metal is still in debate.^{8,11,12} The seemingly different activities of INLPs from environmental and infectious bacteria prompted the need for scrutinizing these BGCs for elucidating different INLP chemical structures and their biosynthetic pathways. Since the INLP metabolites were indicated to modulate host–pathogen interactions and disease outcome in *Mtb*,^{8,11–21} a thorough understanding of INLP biosynthesis in pathogenic mycobacteria would further facilitate the study of INLP-mediated virulence and reveal potential drug targets to combat mycobacterial infections.

The activity of the five core enzymes for INLP biosynthesis in *Streptomyces*, represented by ScoA–E from *Streptomyces coeruleorubidus*, has been well studied using biochemical analyses (Figure 1B).^{6,8,22–24} The biosynthetic pathway starts with the activation and loading of crotonic acid to an acyl carrier protein (ACP), ScoB, catalyzed by an acyl-ACP ligase, ScoC. A thioesterase homolog, ScoD, next promotes both the β -glycine adduct formation via Michael addition, followed by hydrolytic release from ScoB to form (*R*)-3-[(carboxymethyl)-amino]butanoic acid (CABA). ScoE, a non-heme iron(II) and α -ketoglutarate (Fe(II)/ α -KG)-dependent oxidase/decarboxylase, then catalyzes isonitrile formation from CABA to generate (*R*)-3-isocyanobutanoic acid (INBA), which is reactivated and loaded onto ScoB by the promiscuous ScoC before the NRPS. Lastly, ScoA promotes INLP formation by condensing the isonitrile ACP-bound intermediate to both amino groups of Lys and reductively releases the INLP alcohol product. Not much is known about the activity of the five homologous enzymes for INLP biosynthesis in mycobacteria, although it is suggested that mycobacterial enzymes differ from those of *Streptomyces* on the fatty-acyl chain length specificity based on the biochemical and structural analyses, heterologous expression in *Escherichia coli*, and identification of related kupyaphores from *Mtb*.^{8,11,25–27} Interestingly, the recent study of kupyaphore biosynthesis in *Mtb* indicated that Rv0097, the ScoE homologue, promotes isonitrile formation on an ACP-bound substrate instead of a small molecule,¹¹ raising additional questions on the activity and substrate specificity of this unique family of isonitrile-forming enzymes.

In the present work, we successfully produce INLPs through in vitro total biosynthesis using enzymes from *Mtb* and *M. marinum*. We scrutinize the activity and substrate specificity of individual enzymes, with a particular focus on the isonitrile-forming enzymes, Rv0097 and MmaE. We demonstrate that like ScoE, Rv0097 and MmaE recognize free acid substrates and further identify a key residue that dictates the varied fatty-acyl chain length specificity between *Streptomyces* and *Mycobacterium*.

MATERIALS/EXPERIMENTAL DETAILS

Commercial Materials.

Phusion High-Fidelity PCR Master Mix with HF buffer (Thermo Scientific) was used for PCR reactions. FastDigest restriction enzymes were purchased from Thermo Scientific. Oligonucleotides were purchased from Integrated DNA Technologies. All the chemicals used in this work were purchased from Sigma-Aldrich, Fisher Scientific, or Alfa Aesar, unless otherwise noted. 3-Amino-decanoic acid hydrochloride (purity: 95%) was purchased from Enamine.

Construction of Plasmids for Expression in *E. coli*.

Individual genes were PCR-amplified from genomic DNA (*M. tuberculosis* H37Rv, *M. marinum* M, and *Streptomyces coreuleorubidus* NRRL18370) and cloned into pET30, pET24b+, or pETDuet through restriction enzyme digestion (Thermo Fisher) and ligation with NEBuilder HiFi DNA Assembly (New England Biolabs). The primers and vectors used in this study are reported in Tables S1 and S2, respectively. Plasmids were extracted using a Zyppy Miniprep Kit (Zymo Research) and confirmed by DNA sequencing at the UC Berkeley Sequencing Facility.

Site Directed Mutagenesis.

ScoE_F239A and Rv0097_G204F were constructed with the Agilent Quick-Change II Site Directed Mutagenesis kit by following the manufacturer's protocol with the primers listed in Table S1. pET30-ScoE and pET24b+-Rv0097 were utilized as templates. The introduction of point mutations was confirmed with DNA sequencing to yield pET30-ScoE_F239A and pET24b +Rv0097_G204F. F239A was constructed instead of F239G since amino substitutions to Gly have previously been linked to protein destabilization due to an increase in the entropy of folding.^{28,29}

Expression and Purification of Recombinant Proteins.

The expression and purification of all proteins follow the same general procedure, but MmaE/Rv0097 purification was conducted using a similar procedure performed on their homolog, ScoE.²²⁻²⁴ BL21 Star (DE3) competent cells were inoculated (2% inoculum ratio) to 1 L of TB or LB in a shake flask containing 50 µg/mL of kanamycin. Note that the BAP1-competent cells were used for the expression and purification of Rv0100, ScoB, and MmaA to yield holo-ACP proteins. The cells were grown at 37 °C at 250 rpm to an OD₆₀₀ of 0.6. The cells were then cooled on ice for 10 min and induced with 250 µM isopropyl-β-D-galactopyranoside for 16 h at 16 °C and 250 rpm. Cells were harvested by centrifugation (6371g, 4 °C, 15 min), resuspended in 30 mL of lysis buffer [50 mM N-(2-hydroxyethyl)piperazine-N'-ethanesulfonic acid (HEPES) pH 8.0, 500 mM NaCl, and 5 mM imidazole], and lysed by sonication on ice. Cellular debris was removed by centrifugation (27,216g, 4 °C, 45 min), and the supernatant was filtered with a 0.45 µm filter before batch binding. Ni-NTA resin (Qiagen) was added to the filtrate at 3 mL/L of culture, followed by incubation for 1 h at 4 °C. The protein-resin mixture was loaded onto a gravity flow column, in which the flowthrough was discarded. The column was then

washed with approximately 30 mL of wash buffer (50 mM HEPES pH 8.0, 100 mM NaCl, and 20 mM imidazole). Proteins were eluted in approximately 15 mL of elution buffer (50 mM HEPES pH 8.0, 100 mM NaCl, and 250 mM imidazole). The entire process was monitored with a Bradford assay. MmaE/Rv0097/ScoE was concentrated to 10 mL using a 10 kDa Amicon spin filter and subsequently dialyzed using a 10 kDa Slide-A-Lyzer cassette overnight in 1 L of dialysis buffer [50 mM HEPES pH 8.0, 100 mM NaCl, and 1 mM ethylenediaminetetraacetic acid (EDTA)]. The dialysis buffer was changed twice during the overnight period (every 2 h). MmaE/Rv0097/ScoE was concentrated using a 10 kDa Amicon spin filter to 40 mg/mL (with 10% v/v glycerol). All other proteins presented in this study were concentrated and exchanged into exchange buffer (25 mM HEPES pH 8.0 and 100 mM NaCl) using Amicon ultrafiltration units. After two rounds of buffer exchange and concentration, the purified enzyme was removed, and glycerol was added to a final concentration of 10% (v/v). The enzymes were flash-frozen in liquid nitrogen and stored in 30 μ L beads at -80°C . The presence and purity of purified proteins were assessed using SDS-PAGE, and their concentrations were determined using a NanoDrop UV-vis spectrophotometer (Thermo Fisher).

The approximate molecular weights and protein yields are as follows: MmaA (149 kDa, 12 mg/L from LB, Uniprot: B2HKL9), MmaE (34 kDa, 25 mg/L from TB, Uniprot: B2HKM3), ScoB (12 kDa, 15 mg/L from LB, NCBI: AJA05937.1), ScoC (57 kDa, 18 mg/L from LB, NCBI: AJA05936.1), ScoD (19 kDa, 45 mg/L from LB, GenBank: [OL448874](#)), ScoE (37 kDa, 10 mg/L from TB, Uniprot: A0A3B6UEU3), ScoE_F239A (37 kDa, 9 mg/L from TB), Rv0097 (34 kDa, 10 mg/L from TB, Uniprot: P9WG83), Rv0097_G204F (34 kDa, 9.5 mg/L from TB), Rv0098 (27 kDa, 25 mg/L from LB, Uniprot: P9WM66), Rv0099 (60 kDa, 38 mg/L from LB, Uniprot: P9WQ54), and Rv0100 (10 kDa, 13 mg/L from LB, Uniprot: P9WM65).

Reconstitution of Non-Heme Iron(II) and α -KG-dependent Dioxygenases to Yield Holo-Enzymes.

A Bio-Rad Bio-Gel P-6 gel column was equilibrated in exchange buffer (50 mM HEPES pH 8.0 and 100 mM NaCl). MmaE/Rv0097/ScoE was desalted to remove EDTA by following the manufacturer's protocol. The enzyme was immediately added to the biochemical assay and supplemented with ammonium iron(II) sulfate hexahydrate, matching 90% of the protein concentration as previously described.^{23,24}

Liquid Chromatography–High-Resolution Mass Spectrum Analysis of Rv0100-Bound Biosynthetic Intermediates.

Reactions were performed at room temperature for 30 min in 50 μ L of 25 mM ammonium bicarbonate pH 7.8 containing 1 mM 2-decenoic acid, 5 mM ATP, 2 mM MgCl_2 , 20 μ M Rv0099, and 50 μ M Rv0100. After the 30 min incubation period, the reaction was diluted with four volumes of purified water and chilled on ice to slow further reaction progress. The diluted reaction mixture was immediately filtered by a 0.45 μ m polyvinylidene difluoride (PVDF) filter, and 15 μ L was promptly injected onto an Agilent Technologies 6545 Q-TOF liquid chromatography (LC)–mass spectrometry (MS) equipped with a Phenomenex Aeris 3.6 μ m Widepore XB-C18 column ($2.1 \times 100 \text{ mm}^2$). Using a water/acetonitrile mobile phase

with 0.1% (v/v) formic acid, analysis was performed with a linear gradient of 30–50% acetonitrile at a flow rate of 0.25 mL/min. The molecular masses of proteins observed during electrospray ionization were determined using ESIprot to deconvolute the array of observed charge state spikes.³⁰ For phosphopantetheine (Ppant) ejection assays, the same conditions were used, but the source voltage was increased from 75 to 250 V to increase fragmentation of the phosphodiester bond covalently linking the Ppant prosthetic to a holo-ACP.

LC-HRMS Analysis of 3-[(Carboxymethyl)amino]-decanoic Acid Production by Rv0098–0100.

Reactions were performed at room temperature for 30 min, 1, 1.5, and 2 h in 50 μ L of 25 mM ammonium bicarbonate pH 7.8 containing 1 mM 2-decenoic acid, 1 mM glycine, 5 mM ATP, 2 mM MgCl₂, 10 μ M Rv0099, 20 μ M Rv0100, and 30 μ M Rv0098. After the incubation period, the reaction was diluted with four volumes of purified water and chilled on ice to slow further reaction progress. The diluted reaction mixture was immediately filtered by a 0.45 μ m PVDF filter, and 15 μ L was analyzed with LC-high-resolution mass spectrum (HRMS). Using a water/acetonitrile mobile phase with 0.1% (v/v) formic acid, analysis was performed with a linear gradient of 30–50% acetonitrile at a flow rate of 0.25 mL/min. Critically, 3-[(carboxymethyl)amino]decanoic acid (CADA)-*S*-Rv0100 was not detected from the time course experiment and an identical biochemical assay was conducted with a 30 min incubation time, but was quenched with 200 μ L of cold methanol, gently mixed, vortexed, and centrifuged for 10 min to remove aggregated protein. LC–HRMS analysis was conducted on an Agilent Technologies 6545 Accurate-Mass QTOF LC–MS instrument and an Eclipse Plus C18 column (100 \times 4.6 mm). Chromatography was performed using a linear gradient of 2–98% acetonitrile (vol/vol) with 0.1% formic acid over 20 min in water with 0.1% formic acid at a flow rate of 0.5 mL/min. CADA production was confirmed subject to negative controls and compared to a synthetic standard. The calculated *m/z* for CADA ($[M + H]^+ = 246.1700$) was utilized for this analysis (observed: 246.1695, 2 ppm error). Furthermore, utilization of ¹⁵N-glycine, 1-¹³C-glycine, and 2-¹³C-glycine led to the expected mass spectral shift. These results demonstrate that Rv0098 adds glycine to 2-decenoyl-*S*-Rv0100 and hydrolyzes the ACP-bound intermediate to form CADA. Similar assays were conducted with different α,β -unsaturated fatty acids. ScoB-D and Rv0098–0100 were utilized for C4–C8 and C12–C16 α,β -unsaturated fatty acids, respectively.

LC–HRMS Analysis of Isonitrile Tetrazine Click Reactions.

A 100 μ L biochemical assay consisting of 50 mM HEPES pH 8.0, 1 mM CABA/CADA, 2 mM α -KG, 100 μ M apo-ScoE/MmaE/Rv0097, and 90 μ M (NH₄)₂Fe(SO₄)₂ was incubated at room temperature for 10 min. The enzymatic reaction was quenched with 200 μ L of 667 μ M 3,6-di(pyridine-2-yl)-1,2,4,5-tetrazine (Py-tetrazine) dissolved in cold methanol, gently mixed, and incubated for 1 h at room temperature. The quenched reaction mixture was further vortexed and centrifuged for 10 min to remove aggregated protein. LC–HRMS analysis was conducted on an Agilent Technologies 6545 Accurate-Mass QTOF LC–MS instrument and an Eclipse Plus C18 column (100 \times 4.6 mm). Chromatography was performed using a linear gradient of 10–50% acetonitrile (vol/vol) with 0.1% formic acid over 12 min in water with 0.1% formic acid at a flow rate of 0.5 mL/min. The production of isonitrile was determined by looking for the formation of 3,5-di(pyridine-2-

yl)-1*H*-pyrazol-4-amine (Py-AP) and comparing its retention time and mass spectrum with a standard. The Py-AP standard was synthesized and characterized by NMR as previously described¹⁰ and was observed with $[M + H]^+$: 238.1088 (calculated $[M + H]^+$: 238.1086, 0.8 ppm error). Negative controls omitting primary substrate, α -KG, and enzyme were also conducted.

LC–HRMS Analysis of INDA and Succinate Production by Rv0097 and MmaE.

Reactions were performed at room temperature for 15 min in 100 μ L of 50 mM HEPES pH 8 containing 1 mM CADA, 2 mM α -KG, 100 μ M Rv0097/MmaE, and 90 μ M $(NH_4)_2Fe(SO_4)_2$. The reactions were subsequently quenched with 200 μ L of cold methanol and analyzed with LC–HRMS. Chromatography was performed using a linear gradient of 10–50% acetonitrile (vol/vol) with 0.1% formic acid over 12 min in water with 0.1% formic acid (vol/vol) at a flow rate of 0.5 mL/min. Extracted ion chromatograms (EICs) for INDA and succinate were generated using the following *m/z*: $[M - H]^- = 196.1343$ for INDA (observed: 196.1341, 1 ppm error) and $[M - H]^- = 117.0193$ for succinate (observed: 117.0195, 1.7 ppm error), respectively. Negative controls were performed, and enzymatic products were compared to a synthetic INDA standard and commercially purchased succinate.

LC–HRMS Analysis of INDA-S-Rv0100.

Reactions were performed at room temperature for 30 min in 50 μ L of 50 mM ammonium bicarbonate pH 7.8 containing 1 mM CADA, 2 mM α -KG, 5 mM ATP, 2 mM $MgCl_2$, 100 μ M Rv0097, 90 μ M $(NH_4)_2Fe(SO_4)_2$, 20 μ M Rv0099, and 50 μ M Rv0100. After the 30 min incubation period, the reaction was diluted with four volumes of purified water and chilled on ice to slow further reaction progress. The diluted reaction mixture was immediately filtered by a 0.45 μ m PVDF filter, and 15 μ L was analyzed with LC–HRMS. Using a water/ acetonitrile mobile phase with 0.1% (v/v) formic acid, analysis was performed with a linear gradient of 30–50% acetonitrile at a flow rate of 0.25 mL/min. The INDA-S-Rv0100 product was confirmed by performing an assay containing 50 μ L of 25 mM ammonium bicarbonate pH 7.8 containing 1 mM INDA, 5 mM ATP, 2 mM $MgCl_2$, 20 μ M Rv0099, and 50 μ M Rv0100.

LC–HRMS Analysis of Isonitrile Species from Coupled Assays.

CABA/CADA analogues were synthesized enzymatically as mentioned in the previous section. After the 30 min incubation period, the enzymatic assay was combined with 50 μ L of 50 mM HEPES pH 8 containing 2 mM α -KG, 100 μ M Rv0097/MmaE/ScoE, and 90 μ M $(NH_4)_2Fe(SO_4)_2$. After a 15 min incubation period, the reactions were subsequently quenched with 200 μ L of cold methanol and analyzed with LC–HRMS as previously described.

Determination of Kinetic Parameters of Rv0097 toward CADA.

Biochemical assays (100 μ L) were performed in triplicate containing 50 mM HEPES pH 8.0, 5 mM α -KG, 50 μ M apo-Rv0097, and 45 μ M $(NH_4)_2Fe(SO_4)_2$. The reactions were initiated by adding α -KG, and CADA was supplied at final concentrations of 50 μ M, 150

μM , 400 μM , 750 μM , 1.2 mM, 2 mM, and 4 mM. After incubation, the enzymatic reaction was quenched with 200 μL of 667 μM 3,6-di(pyridine-2-yl)-1,2,4,5-tetrazine (Py-tetrazine) dissolved in cold methanol, gently mixed, and incubated for 1 h at room temperature. The subsequent reactions were centrifuged to remove protein debris and the supernatant was analyzed with LC–HRMS. Time points were taken at 30 s, 1 min, 2 min, 5 min, and 10 min to determine the initial velocity of INDA formation. The product concentration was estimated by constructing a standard curve of Py-AP by analysis of standards containing 100 μL of 50 mM HEPES pH 8.0 and varying amounts of Py-AP that were subsequently quenched with 200 μL of 667 μM Py-tetrazine dissolved in cold methanol. Chromatography was performed using a linear gradient of 10–50% acetonitrile (vol/vol) with 0.1% formic acid over 12 min in water with 0.1% formic acid at a flow rate 0.5 mL/min. Kinetic parameters were then calculated using GraphPad Prism.

LC–HRMS Analysis of INLP Production by Rv0097/MmaE with Rv0098–0100 and MmaA.

Reactions were performed at room temperature for 2 h in 100 μL of 50 mM HEPES pH 8.0 containing 5 mM α -KG, 2 mM 2-decenoic acid, 5 mM Gly, 10 mM NADPH, 10 mM lysine, 10 mM ATP, 10 mM MgCl_2 , 45 μM $(\text{NH}_4)_2\text{Fe}(\text{SO}_4)_2$, 30 μM Rv0098, 50 μM Rv0099, 50 μM Rv0100, 50 μM Rv0097/MmaE, and 50 μM MmaA. The reactions were subsequently quenched with 200 μL of cold methanol and analyzed with LC–HRMS. Chromatography was performed using a linear gradient of 2–98% acetonitrile (vol/vol) with 0.1% formic acid over 30 min in water with 0.1% formic acid (vol/vol) at a flow rate of 0.5 mL/min. The INLP product ($[\text{M} + \text{H}]^+$: 505.3749) was detected subject to negative controls (observed: 505.3764, 3.0 ppm error).

Proteins Used in This Study.

MmaA (Uniprot: B2HKL9), MmaE (Uniprot: B2HKM3), ScoB (NCBI: AJA05937.1), ScoC (NCBI: AJA05936.1), ScoD (GenBank: [OL448874](#)), ScoE (Uniprot: A0A3B6UEU3), Rv0097 (Uniprot: P9WG83), Rv0098 (Uniprot: P9WM66), Rv0099 (Uniprot: P9WQ54), and Rv0100 (Uniprot: P9WM65).

RESULTS/DISCUSSION

Total Biosynthesis of INLPs Using Mycobacterial Enzymes.

Previous heterologous expression of *mmaA-E* or *Rv0097–0100-mmaA* in *E. coli* led to the production of the same INLPs upon feeding of medium-chain α,β -unsaturated fatty acids, indicating the interchangeability among the encoding four enzymes from these two *Mycobacterium* species, except the NRPSs.⁸ To further confirm these enzyme activities, we sought to first reconstitute INLP biosynthesis in vitro using purified mycobacterial enzymes from *E. coli* (Figure S1). MmaA, the single-module NRPS from *M. marinum*, was used throughout since the di-module NRPS of *Mtb* (Rv0101) could not be functionally expressed in *E. coli*. A coupled biochemical assay containing enzymes Rv0097–0100 and MmaA, together with 2-decenoic acid, ATP, Gly, α -KG, Lys, and NADPH, generated **INLP6**, which was reported previously from heterologous expression in *E. coli* (Figures 2 and S2).⁸ **INLP6** was also produced from coupled assays in which Rv0097 was replaced by MmaE (91% sequence identity/97% similarity), further showing the equivalent activity of Rv0097

and MmaE (Figure 2). The successful total biosynthesis of **INLP6** set the stage for the subsequent biosynthetic pathway delineation.

Rv0098 is Dual-Functional Thioesterase that Generates a Fatty Acyl β -Gly Acid.

Rv0098/MmaD was proposed to generate a fatty acyl β -Gly adduct to be served as the substrate for Rv0097/MmaE, but it is questionable whether the Gly adduct appears as the free acid or remains on the ACP. To reconstitute the activity of Rv0098, its substrate 2-decenoyl-*S*-Rv0100 was generated from the Rv0099-catalyzed reaction containing holo-Rv0100, 2-decenoic acid, and ATP. The formation of 2-decenoyl-*S*-Rv0100 was confirmed based on the intact protein HRMS analysis and a Ppant ejection assay (Figures 3A and S3A). Addition of Rv0098 and Gly to the coupled assay resulted in consumption of 2-decenoyl-*S*-Rv0100 compared to negative controls, but we were unable to detect 3-[(carboxymethyl)amino]decanoyl-*S*-Rv0100 as previously proposed by Mehdiratta et al. (Figure S3B).¹¹ Analysis of the Rv0098-Rv0100 assay supernatant by LC–HRMS resulted in detection of CADA in comparison with a synthetic standard (Figures 3B and S4–S6). Rv0098–Rv0100 assays using ¹⁵N-glycine, 1-¹³C-glycine, and 2-¹³C-glycine led to the expected mass spectral shifts, further confirming the production of CADA product in the supernatant (Figures 3B and S7). CADA was previously suggested to be produced by the MmaBCD assay and readily released from ACP by hydrolysis, consistent with the results from the Rv0098–Rv0100 assay.⁸ It is notable that the hydrolytic activity of Rv0098 was well established via biochemical studies using various acyl-CoA compounds as substrates.²⁵ We, therefore, propose that similar to ScoD (35% sequence identity/52% similarity) and other homologues from *Streptomyces* such as SAV606 (36% sequence identity/54% similarity) and CmiS1 (36% sequence identity/52% similarity),^{31,32} Rv0098/MmaD catalyzes both the Michael addition of Gly to an α,β -unsaturated fatty acyl-ACP substrate and subsequent hydrolysis to yield a fatty acyl β -Gly acid (Figure 3). We suspect that Rv0098 promotes these two reactions with a conserved His residue in the active site that plays a critical role in both the Michael addition and hydrolysis via a water molecule based on a sequence and structural alignment of Rv0098 and SAV606 (Figure S8).³¹ Additional coupled assays using α,β -unsaturated fatty acid's varying chain lengths further demonstrated that Rv0098–0100 produced medium- to long-chain fatty acyl β -Gly acids, different from *Streptomyces* homologues, which appeared to generate a short- to medium-chain length products (Figures 3C and S9). This result was consistent with previous reports stating that Rv0098 promoted the hydrolysis of C4–C18 acyl-CoA substrates with a preference toward long-chain fatty acyl groups (>C12), and no activity of Rv0098 was observed for the *N*-acetyl cysteamine (NAC)-thioester of crotonic acid and minor products were obtained with octenoic acids for Gly adduct formation.^{11,25}

Rv0097 Catalyzes Isonitrile Formation on a Free Acid without ACP Requirement.

Once CADA was confirmed as the reaction product from the coupled Rv0098–0100 assay with 2-decenoic acid, we next probed the activity of Rv0097 on CADA.

Rv0097 was purified from *E. coli* by removal of co-purified metals and reconstituting its activity with fresh Fe(II) before each enzymatic assay. An in vitro biochemical assay containing CADA, α -KG, Rv0097, and Fe(II) led to the production of succinate

and 3-isocyanodecanoic acid (INDA) in comparison to synthetic standards (Figures 4A and S10–S13). In addition, using a reported derivatization method for isonitrile detection and quantification,^{10,23,24} the addition of 3,6-di(pyridine-2-yl)-1,2,4,5-tetrazine (Py-tetrazine) led to the formation of 3,5-di(pyridine-2-yl)-1*H*-pyrazol-4-amine (Py-AP), further confirming the production of an isonitrile compound (Figure S13). The kinetic parameters of Rv0097 for CADA were then determined ($K_M = 405 \pm 33 \mu\text{M}$, $k_{\text{cat}} = 3.27 \pm 0.37 \text{ min}^{-1}$) (Figure 4B). The observed large K_M for CADA is most likely attributed to not being the most preferred chain length for Rv0097.¹¹ The catalytic mechanism of Rv0097 likely mirrors the mechanism of its homologue ScoE (45% sequence identity/61% similarity), for which we and other researchers recently characterized (Figure S14).^{23,24,33,34} Isonitrile formation requires a four-electron oxidation of the primary substrate, thus indicating that two α -KG half reactions are required for isonitrile formation. The pathway commences with the first α -KG half reaction, generating the first Fe(IV)=O species that abstracts a hydrogen from the C11 position of CADA, followed by a hydroxyl rebound that generates C11–OH CADA. A catalytic base near the active site aids in the dehydration of this enamine to generate imine-CADA. Lastly, the second α -KG half reaction generates the second Fe(IV)=O species that helps promote radical-based oxidative transformation on imine-CADA to synthesize CO₂ and isonitrile.

The successful synthesis of INDА from CADA catalyzed by Rv0097 established that Rv0097 catalyzes isonitrile formation on a free acid substrate without the requirement of ACP, different from a recent hypothesis that the ACP-bound substrate is required for the activity of Rv0097.¹¹ INDА was expected to be reactivated for NRPS-promoted condensation, and we thus probed the activity of Rv0099 again to see if it is capable of activating and loading INDА onto Rv0100, similar to the promiscuous activity of ScoC.²² A biochemical assay with INDА, ATP, Rv0099, and Rv0100 yielded the expected product, INDА-*S*-Rv0100, based on the intact protein HRMS analysis and a Ppant ejection assay (Figures 4C and S15). In addition, the same product of INDА-*S*-Rv0100 was formed in the coupled assay with CADA, α -KG, ATP, and enzymes Rv0097, Rv0099, and Rv0100 (Figure 4C), but Rv0099 failed to catalyze the loading of CADA to Rv0100 (Figure S15), further arguing against the possibility of Rv0097 working on an ACP substrate. These results unequivocally confirmed that Rv0097 recognizes a free acid substrate to yield an isonitrile acid, which is then reactivated by the promiscuous acyl-ACP ligase Rv0099 (Figure 4). Rv0097 may have relaxed substrate specificity toward the fatty carboxylate modification as the corresponding NAC-thioester seemed to be recognized by Rv0097 to form an isonitrile NAC-thioester product.¹¹

Probing the Substrate Specificity of Isonitrile-forming Enzymes from *Streptomyces* and *Mycobacterium*.

The fatty-acyl chain length specificity of enzymes upstream of the isonitrile-forming enzyme is consistent with the chain length of observed metabolites from *Streptomyces* and *Mycobacterium* (Figures 1 and 3).^{8–10} It is thus interesting to probe whether the isonitrile-forming enzymes, such as ScoE and Rv0097/MmaE, serve as another gate-keeping enzyme for chain length. After reconstituting the activity of Rv0097 with CADA (C10), we performed biochemical assays with ScoE and MmaE with CADA to test for INDА

production. INDA was only detected from the assay with MmaE (Figure 5A). On the other hand, Rv0097 and MmaE were unable to recognize the native substrate of ScoE (CABA, C4) (Figure 5A), indicating that isonitrile-forming enzymes from *Mycobacterium* and *Streptomyces* possess different chain length specificities.

To further probe the substrate length scope, coupled assays were performed to enzymatically generate CADA analogues spanning from C4 to C16 with respect to their fatty acyl chain (Figures 3C and S9). These CADA analogues were then tested for their recognition by Rv0097, MmaE, and ScoE, respectively. ScoE was found to recognize substrates with fatty acyl chains C4–C8 with a preference toward C4, while Rv0097/MmaE recognized substrates with C8–C16 fatty acyl chains with a preference toward >C10 (Figure 5B). The observed different chain-length specificity of isonitrile-forming enzymes agreed well with the chemical structures of the isonitrile metabolites isolated from *Streptomyces* and *Mtb*, respectively (Figure 1).^{8,9,11}

Single Amino Acid Alteration Relaxes Isonitrile-Forming Enzyme Substrate Specificity.

Considering the different fatty-acyl chain length specificity of Rv0097/MmaE and ScoE, we next sought to obtain molecular insights into potential residue(s) that may confer substrate selectivity for this family of isonitrile-forming enzymes. A sequence alignment revealed several conserved residues that are typical within this enzyme superfamily (Figure 6A). Fe(II)/ α -KG dioxygenases possess a conserved activation mechanism involving mononuclear Fe(II) coordinated to a conserved 2-histidine-1-carboxylate facial triad with α -KG bound to the metal-locofactor in a bidentate configuration, with the exception that the carboxylate ligand replaced with alanine/glycine for the case Fe(II)/ α -KG halogenases.^{24,35–37} Rv0097 possesses a 2-His-1-Asp facial triad based on the sequence alignment consisting of His97, Asp99, and His260 that coordinate to Fe(II) during catalysis. Based on our recent structures of ScoE with CABA bound, we found that the residues important for CABA binding, such as Lys193, Arg310, and Tyr96 in ScoE, were conserved in Rv0097 as well (Lys158, Arg275, and Tyr65).²³

The side chain of Tyr96 hydrogen bonds with the secondary amine of CABA and has been proposed to act as a catalytic base en route to isonitrile formation.²⁴ One residue of interest from our structure of ScoE_CABA was Phe239, which appears to be located at the vicinity of the active site with the side chain interacting with the fatty-acyl chain of CABA (Figure 6B). Notably, Phe239 was not conserved in Rv0097/MmaE, in which a Gly residue was found (Figure 6A). To probe the importance of the Gly/Phe residue regarding its potential role in dictating fatty-acyl chain specificity, two enzyme variants were expressed and purified for biochemical assays (Rv0097_G204F and ScoE_F239A) (Figure S1). Assays using Rv0097_G204F with CABA or CADA demonstrated nearly equal production of the isonitrile products, albeit at lower amounts compared to the wild-type variant (Figure 6C). This change of substrate recognition of Rv0097 after a single point mutation is likely because the switch to a bulky aromatic group (Phe) potentially interferes with CADA binding due to steric hindrance with the long alkyl chain and aromatic side chain. Similarly, ScoE_F239A switched its preference from CABA to CADA, although the overall synthesis efficiency decreased too (Figure 6D). Altogether, this single amino acid alteration in ScoE

and Rv0097 enabled both enzymes to convert two previously unaccepted substrates into isonitrile products. Considering that the single amino acid alteration of Gly/Phe was not sufficient in a complete switch of chain length specificity of these enzymes, we propose that other residue(s) may also play a role. Further insights into the responsible residue(s) will be facilitated with a substrate bound structure of Rv0097, which is currently in progress.

CONCLUSIONS

In summary, we have elucidated the activity of the five core enzymes in generating INLP metallophores from pathogenic mycobacteria. The pathway commences with an initial loading and activation of a medium-/long-chain length α,β -unsaturated fatty acid (>C10) by Rv0099 onto the ACP, Rv0100 (Figure 1). A thioesterase homolog (Rv0098) then catalyzes both the Michael addition of glycine to the β -position of the α,β -unsaturated fatty acyl-ACP intermediate, followed by the hydrolysis of the ACP to generate a β -glycine adduct attached to a fatty acid (Figure 1). This intermediate is modified by Rv0097, a Fe(II)/ α -KG dioxygenase, which catalyzes isonitrile formation by an oxidative decarboxylation mechanism (Figure 1). The resulting isonitrile is activated again by Rv0099 and loaded onto Rv0100 (Figure 1). In *Mtb*, the ACP-bound isonitrile intermediate would lastly undergo modification by Rv0101, a di-module NRPS, through the incorporation of ornithine, phenylalanine, and a final reductive release to form reported kupyaphores. In *M. marinum*, a single-module NRPS, MmaA would promote the condensation to lysine and reductive release to form INLP, although the native BGC metabolites remain unknown. This work established the catalytic activity of the isonitrile-forming enzyme in pathogenic mycobacteria, which is different from the recent report,¹¹ and further provided molecular insights in different substrate recognition by homologous isonitrile-forming enzymes from environmental and infectious bacteria.

Supplementary Material

Refer to Web version on PubMed Central for supplementary material.

ACKNOWLEDGMENTS

We would like to thank Dr. Jeff Pelton for helping with NMR spectroscopic analysis. This research was financially supported by a grant to W.Z. from the NIH (R01GM136758).

ABBREVIATIONS

α -KG

α -ketoglutarate

Fe(II)/ α -KG dioxygenase

non-heme iron(II) and α -KG-dependent dioxygenase

CABA

(*R*)-3-[(carboxymethyl)amino]butanoic acid

CADA

3-[(carboxymethyl)amino]decanoic acid

Gly

glycine

Lys

lysine

INBA

(*R*)-3-isocyanobutanoic acid

INDA

3-isocyanodecanoic acid

Py-tetrazine

3,6-di(pyridine-2-yl)-1,2,4,5-tetrazine

Py-AP

3,5-di(pyridine-2-yl)-1*H*-pyrazol-4-amine

INLP

isonitrile lipopeptide

LC–HRMS

liquid chromatography–high resolution mass spectrometry

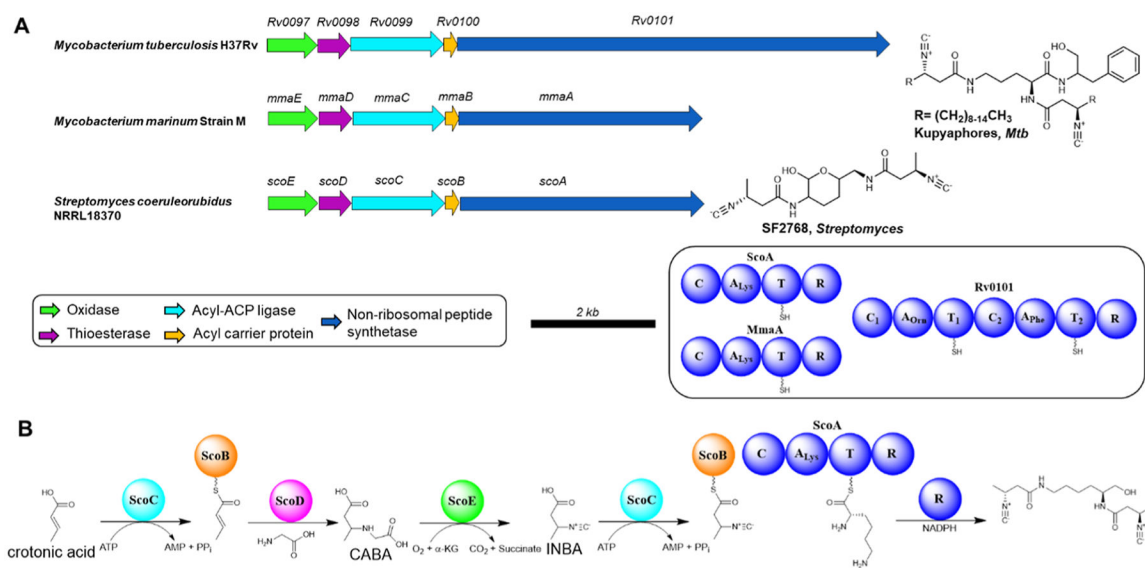
EIC

extracted ion chromatogram

REFERENCES

- (1). O'Brien J; Wright GD An Ecological Perspective of Microbial Secondary Metabolism. *Curr. Opin. Biotechnol* 2011, 22, 552–558. [PubMed: 21498065]
- (2). Newman DJ; Cragg GM Natural Products as Sources of New Drugs from 1981 to 2014. *J. Nat. Prod* 2016, 79, 629–661. [PubMed: 26852623]
- (3). Ren Y; Bai Y; Zhang Z; Cai W; Del Rio Flores A The Preparation and Structure Analysis Methods of Natural Polysaccharides of Plants and Fungi: A Review of Recent Development. *Molecules* 2019, 24, 3122–3126. [PubMed: 31466265]
- (4). Barber CC; Zhang W Small Molecule Natural Products in Human Nasal/Oral Microbiota. *J. Ind. Microbiol. Biotechnol* 2021, 48, 1–12.
- (5). Hu Z; Zhang W Signaling Natural Products from Human Pathogenic Bacteria. *ACS Infect. Dis* 2020, 6, 25–33. [PubMed: 31617342]
- (6). Del Rio Flores ADR; Barber CC; Narayanamoorthy M; Gu D; Shen Y; Zhang W Biosynthesis of Isonitrile- and Alkyne-Containing Natural Products. *Annu. Rev. Chem. Biomol. Eng* 2022, 13, 1–24. [PubMed: 35236086]
- (7). Del Rio Flores A; Twigg FF; Du Y; Cai W; Aguirre DQ; et al. Biosynthesis of Triacsin Featuring an *N*-Hydroxytriazene Pharmacophore. *Nat. Chem. Biol* 2021, 17, 1305. [PubMed: 34725510]
- (8). Harris NC; Sato M; Herman NA; Twigg F; Cai W; Liu J; Zhu X; Downey J; Khalaf R; Martin J; Koshino H; Zhang W Biosynthesis of Isonitrile Lipopeptides by Conserved Nonribosomal Peptide Synthetase Gene Clusters in Actinobacteria. *Proc. Natl. Acad. Sci. U.S.A* 2017, 114, 7025–7030. [PubMed: 28634299]

- (24). Del Rio Flores A; Kastner WD; Du Y; Narayanamoorthy D; Shen Y; Cai W; Vennelakanti V; Zill NA; Dell LB; Kulik B; Zhai R; Kulik JH; Zhang W Probing the Mechanism of Isonitrile Formation by a Non-Heme Iron(II)-Dependent Oxidase/Decarboxylase. *J. Am. Chem. Soc* 2022, 144, 5893–5901. [PubMed: 35254829]
- (25). Wang F; Langley R; Gulten G; Wang L; Sacchettini JC Identification of a Type III Thioesterase Reveals the Function of an Operon Crucial for Mtb Virulence. *Chem. Biol* 2007, 14, 543–551. [PubMed: 17524985]
- (26). Chhabra A; Haque AS; Pal RK; Goyal A; Rai R; Joshi S; Panjkar S; Pasha S; Sankaranarayanan R; Gokhale RS Nonprocessive [2 + 2]e⁻ off-Loading Reductase Domains from Mycobacterial Nonribosomal Peptide Synthetases. *Proc. Natl. Acad. Sci. U.S.A* 2012, 109, 5681–5686. [PubMed: 22451903]
- (27). Liu Z; Ioerger TR; Wang F; Sacchettini JC Structures of Mycobacterium Tuberculosis FadD10 Protein Reveal a New Type of Adenylate-Forming Enzyme. *J. Biol. Chem* 2013, 288, 18473–18483. [PubMed: 23625916]
- (28). Pakula AA; Sauer RT Genetic Analysis of Protein Stability and Function. *Annu. Rev. Genet* 1989, 23, 289–310. [PubMed: 2694933]
- (29). Matthews BW; Nicholson H; Becktel WJ Enhanced Protein Thermostability from Site-Directed Mutations That Decrease the Entropy of Unfolding. *Proc. Natl. Acad. Sci. U.S.A* 1987, 84, 6663–6667. [PubMed: 3477797]
- (30). Winkler R ESIprot: a universal tool for charge state determination and molecular weight calculation of proteins from electrospray ionization mass spectrometry data. *Rapid Commun. Mass Spectrom* 2010, 24, 285–294. [PubMed: 20049890]
- (31). Chisuga T; Miyanaga A; Kudo F; Eguchi T Structural analysis of the dual-function thioesterase SAV606 unravels the mechanism of Michael addition of glycine to an α,β -unsaturated thioester. *J. Biol. Chem* 2017, 292, 10926–10937. [PubMed: 28522606]
- (32). Amagai K; Takaku R; Kudo F; Eguchi T A Unique Amino Transfer Mechanism for Constructing the β -Amino Fatty Acid Starter Unit in the Biosynthesis of the Macrolactam Antibiotic Cremimycin. *ChemBioChem* 2013, 14, 1998–2006. [PubMed: 24014395]
- (33). Chen T; Chen J; Tang Y; Zhou J; Guo Y; Chang W Pathway from N-Alkylglycine to Alkylisonitrile Catalyzed by Iron(II) and 2-Oxoglutarate-Dependent Oxygenases. *Angew. Chem* 2020, 132, 7437–7441.
- (34). Chen T-Y; Zheng Z; Zhang X; Chen J; Cha L; Tang Y; Guo Y; Zhou J; Wang B; Liu H; Chang W Deciphering the Reaction Pathway of Mononuclear Iron Enzyme-Catalyzed N \equiv C Triple Bond Formation in Isocyanide Lipopeptide and Polyketide Biosynthesis. *ACS Catal.* 2022, 12, 2270–2279. [PubMed: 35992736]
- (35). Martinez S; Hausinger RP Catalytic Mechanisms of Fe(II)- and 2-Oxoglutarate-Dependent Oxygenases. *J. Biol. Chem* 2015, 290, 20702–20711. [PubMed: 26152721]
- (36). Blasiak LC; Vaillancourt FH; Walsh CT; Drennan CL Crystal Structure of the Non-Haem Iron Halogenase SyrB2 in Syringomycin Biosynthesis. *Nature* 2006, 440, 368–371. [PubMed: 16541079]
- (37). Neugebauer ME; Kissman EN; Marchand JA; Pelton JG; Sambold NA; Millar DC; Chang MCY Reaction Pathway Engineering Converts a Radical Hydroxylase into a Halogenase. *Nat. Chem. Biol* 2021, 18, 171–179. [PubMed: 34937913]

**Figure 1.**

Biosynthesis of INLPs from actinobacteria. (A) Schematic of the conserved INLP biosynthetic operons with known metabolites. (B) Activity of ScoA-E for INLP biosynthesis. Domain abbreviations: C, condensation; A, adenylation; R, reduction; T, thiolation.

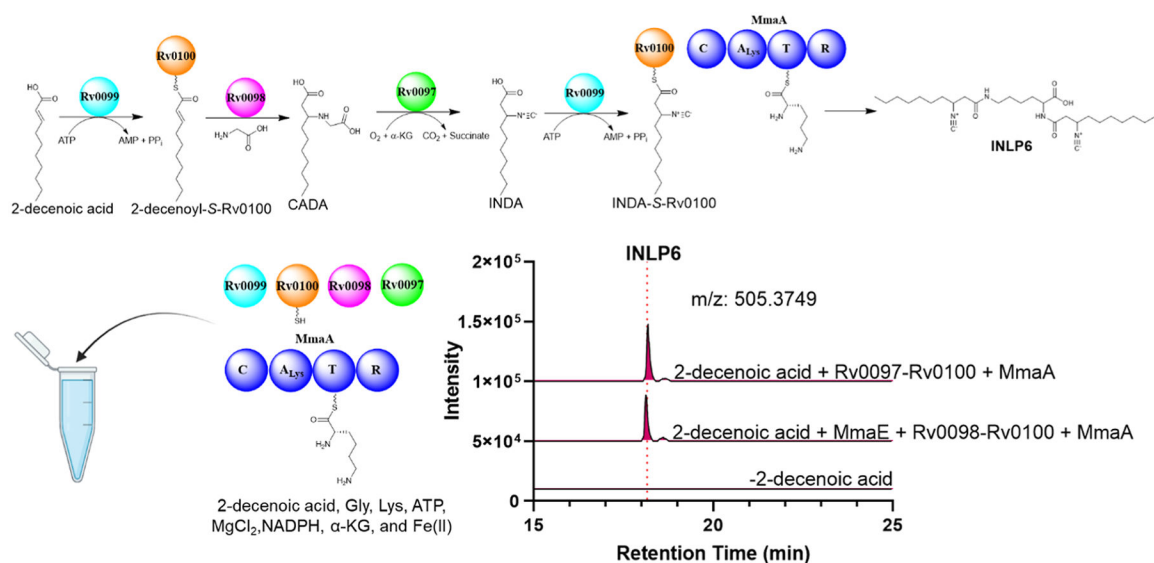


Figure 2.

Total in vitro synthesis of INLP using mycobacterial enzymes. EICs showing production of **INLP6** from a biochemical assay analyzed by LC–HRMS that contains mycobacterial enzymes, 2-decenoic acid, Gly, α -KG, Lys, ATP, and NADPH. **INLP6** is generated from spontaneous hydrolysis from the NRPS as previously reported.⁸ MmaE/Rv0097 (97% sequence similarity) can be used interchangeably to generate **INLP6**. A 10 ppm error mass tolerance was used for each trace.

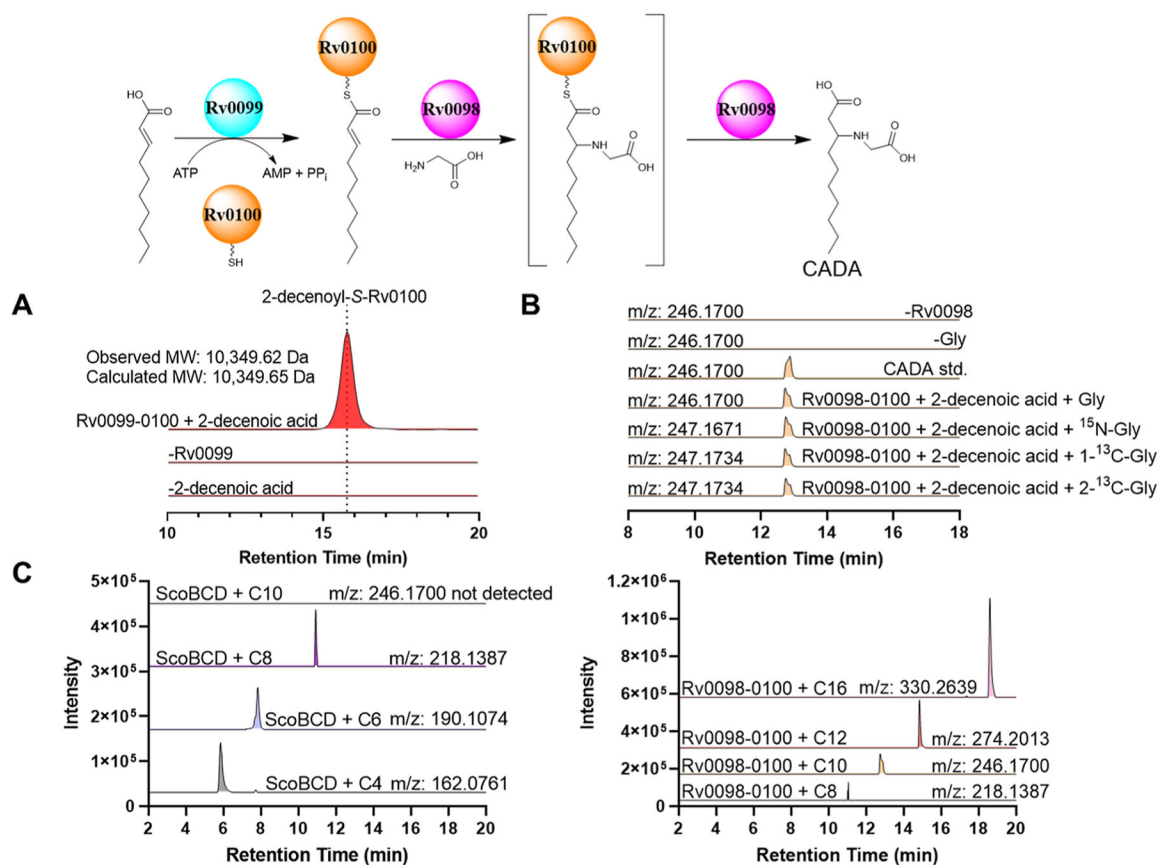
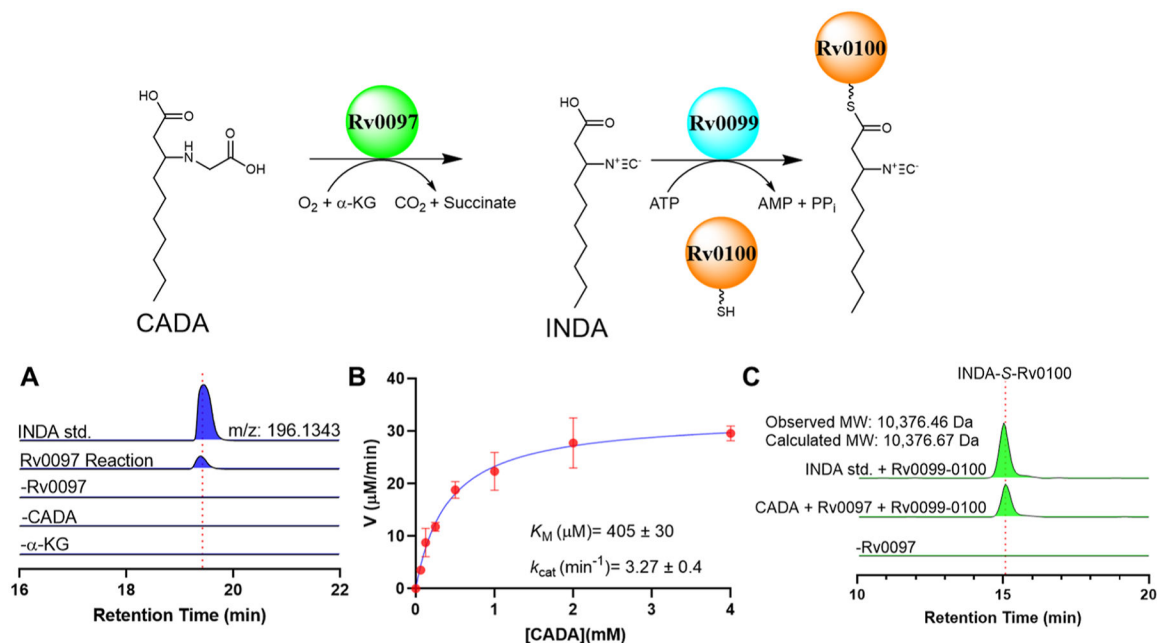
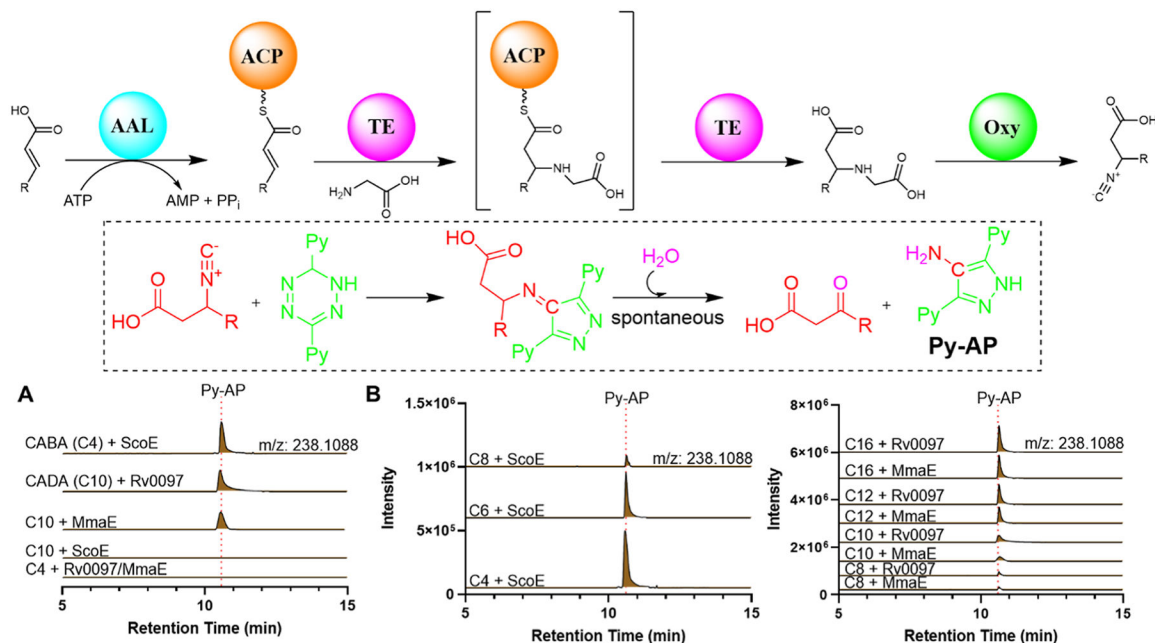


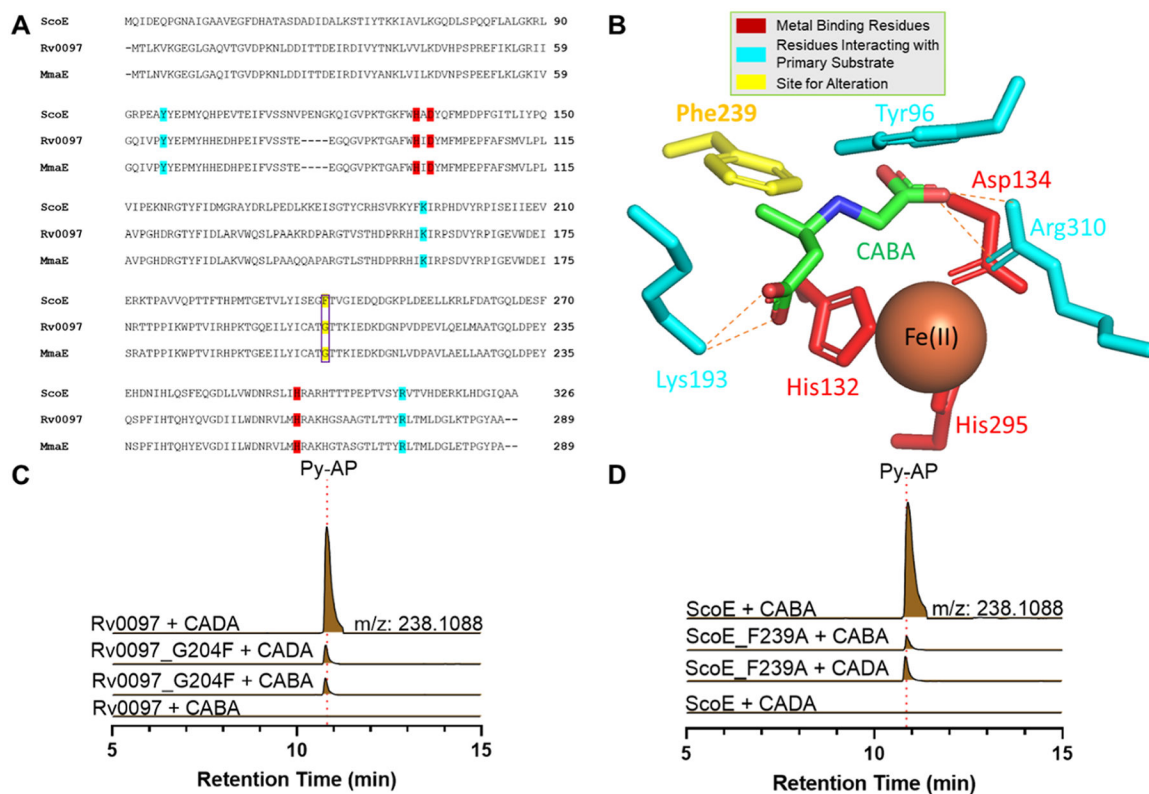
Figure 3. Biochemical analysis of Rv0098–0100. (A) EICs demonstrating production of 2-decenoyl-S-Rv0100 (+11 charge) from a coupled Rv0099–0100 assay with 2-decenoic acid. (B) EICs demonstrating production of CADA from analysis of the reaction supernatant in comparison to a synthetic standard. Utilization of labeled glycine substrates resulted in the expected mass spectral shifts, respectively. (C) EICs demonstrating enzymatic production of fatty-acyl chain substrates bearing a β -glycine adduct with varying fatty-acyl chain length. A 10 ppm mass error tolerance was used for each trace.

**Figure 4.**

In vitro reconstitution of Rv0097 and loading of INDA onto Rv0100. (A) EICs showing production of INDA from a biochemical assay containing CADA, α -KG, Rv0097, and Fe(II) subject to negative controls and in comparison to a synthetic standard. (B) Rv0097 kinetic parameters for CADA in INDA formation at room temperature. The data points and error bars represent the average and standard deviation from three independent experiments, respectively. (C) EICs demonstrating production of INDA-S-Rv0100 (+11 charge) along with its deconvoluted mass from a coupled Rv0097 and Rv0099–0100 assay with CADA in comparison to an INDA standard loaded onto Rv0100. A 10 ppm mass error tolerance was used for each trace.

**Figure 5.**

Fatty-acyl chain length specificity of Fe(II)/ α -KG dioxygenases involved in isonitrile synthesis. (A) EICs demonstrating production of Py-AP from biochemical assays utilizing combinations of CABA/CADA with Rv0097/MmaE/ScoE. Overall, ScoE was only able to recognize CABA (C4), while the mycobacterial enzymes (Rv0097 and MmaE) recognized CADA (C10), thus demonstrating distinct fatty-acyl chain length specificity. (B) EICs demonstrating production of Py-AP from ScoE biochemical assays using enzymatically prepared C4–C8 fatty-acyl chain length substrates containing a β -glycine adduct. ScoE was able to recognize C4–C8 substrates with a preference for C4. (C) EICs demonstrating production of Py-AP from Rv0097/MmaE biochemical assays using enzymatically prepared C8–C16 fatty-acyl chain length substrates containing a β -glycine adduct. Both enzymes were able to recognize C8–C16 substrates with a preference for >C10. A 10 ppm mass error tolerance was used for each trace.

**Figure 6.**

Substitution of a single amino acid residue relaxes fatty acyl chain length specificity of Rv0097 and ScoE. (A) Sequence alignment of ScoE, Rv0097, and MmaE with the metal-binding residues, primary substrate-interacting residues, and our site for alteration highlighted in red, cyan, and yellow, respectively. (B) Active site of ScoE with CABA, Fe(II), and the key residues highlighted in the sequence alignment (PDB: 6XN6). (C) EICs of Py-AP demonstrating production of isonitrile from biochemical assays of Rv0097_G204F with CABA and CADA, respectively, and subject to controls with wild type Rv0097. (D) EICs of Py-AP demonstrating production of isonitrile from biochemical assays of ScoE_F239A with CABA and CADA, respectively, and subject to controls with wild type ScoE. A 10 ppm error tolerance was utilized for each trace.